

# FINITE ELEMENT ANALYSIS OF ULTRASONIC PHASED ARRAY INSPECTIONS ON ANISOTROPIC WELDS

G. Harvey<sup>1</sup>, A. Tweedie<sup>2</sup>, C. Carpentier<sup>3</sup>, P. Reynolds<sup>4</sup>

<sup>1</sup> Weidlinger Associates, Glasgow, UK, G4 0LT

<sup>2</sup> ALBA Ultrasound, Glasgow, UK, G20 0XA

<sup>3</sup> TWI, Cambridge, UK, CB21 6AL

<sup>4</sup> Weidlinger Associates, Mountain View, CA 94040

**ABSTRACT.** This paper describes a theoretical investigation into the behaviour of anisotropic welds under phased array inspection procedures using a 128 element linear array. Two advanced inspection techniques are simulated, and their suitability compared. A finite element (FE) model, configured in PZFlex, is used to represent both the variations in crystal orientation found in a typical anisotropic weld, and also the linear array configuration. Firstly, through transmission spectra of the weld are used to determine the optimum operating frequency and configuration of the array in order to detect a 3mm SDH in the weld. Next, the Full Matrix Capture (FMC) technique is simulated, and an image of the weld constructed using the Total Focussing Method (TFM). This is accomplished by transmitting on each element sequentially, while receiving on the remaining 127 elements. This approach provides spatial averaging over the weld area, reducing the distortion caused by the anisotropic media. Finally, Time Reversal Acoustic (TRA) methods were employed to coherently focus the array at the defect and compensate for the elemental timing variations caused by the complex medium. Results illustrate the potential for inspecting anisotropic welds when using correctly designed arrays and implementing novel inspection procedures.

**Keywords:**

**PACS:**

## INTRODUCTION

The ultrasonic non-destructive inspection of non-homogenous materials presents some well known challenges to the technology. These difficulties become evident when the inspection of austenitic welds via phased arrays is considered. Unlike with isotropic materials, austenitic welds are anisotropic in nature due to the various orientations of the grains in the crystal structure. The differences in orientation of these large grains cause them to act as scatters in the path of the ultrasound, resulting in both increased attenuation of the signal and a distortion of the beam path. Given this, the reflections from the grain structure acts as noise, reducing the sensitivity of the inspection considerably, and the skewing of the beam path gives an erroneous interpretation of defect size and location. Moreover, the alteration of the

beam path prevents the reliable use of conventional delay and sum beamforming techniques.

As transducer technology advancements gradually limit the effect of some of the problems associated with such inspections, new ultrasonic inspection procedures must be formulated to ensure these welds can be inspected with reliability and confidence. Traditional analytical and semi-analytical models can rapidly begin to reach their limits in terms of accuracy and computational capacity when attempting to simulate propagation through complex anisotropic media with small, irregular defects present. A method that can offer a solution to this problem will be an invaluable tool in the development of the next generation of inspection procedures.

This paper describes a theoretical investigation into the behaviour of anisotropic welds under phased array inspection procedures using a 128 element linear array. Two advanced inspection techniques are simulated, and their suitability compared. A finite element (FE) model, configured in PZFlex, is used to represent both the variations in crystal orientation found in a typical anisotropic weld, and also the linear array configuration. Firstly, through transmission spectra of the weld are used to determine the optimum operating frequency and configuration of the array in order to detect a 3mm SDH in the weld. Next, the Full Matrix Capture (FMC) technique is simulated, and an image of the weld constructed using the Total Focussing Method (TFM). This is accomplished by transmitting on each element sequentially, while receiving on the remaining 127 elements. This approach provides spatial averaging over the weld area, reducing the distortion caused by the anisotropic media. Finally, Time Reversal Acoustic (TRA) methods were employed to coherently focus the array at the defect and compensate for the elemental timing variations caused by the complex medium. Results illustrate the potential for inspecting anisotropic welds when using correctly designed arrays and implementing novel inspection procedures.

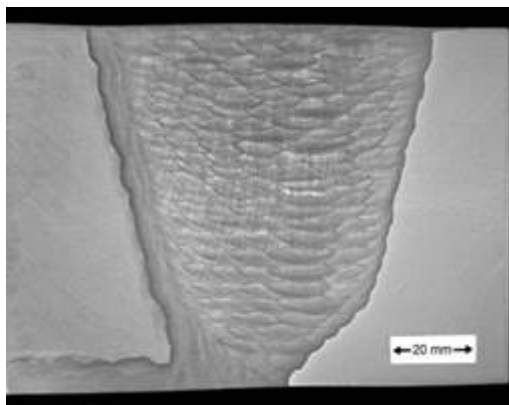


**FIGURE 1.** An austenitic weld showing the buttering and cladding layers. (Reproduced with permission from TWI)

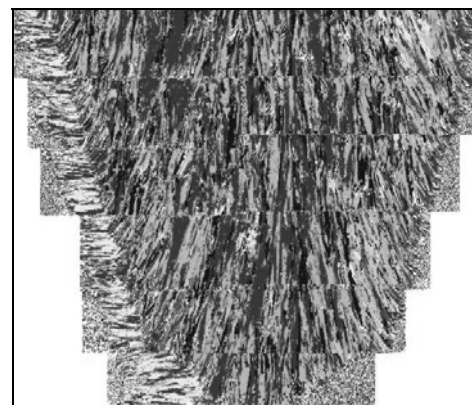


**FIGURE 2.** Processed weld map where color regions represent unique areas of dominant crystal orientation detailed in Table 1. This map is also read into PZFlex to represent the weld. (Reproduced with permission from TWI)

## ANISOTROPIC WELD

To design the inspection with due consideration to the complex material through which the ultrasound has to propagate, the material must be quantified. In the case of the coarse-grained anisotropic austenitic metals, the description must both identify the grain boundaries and evaluate the texture developed in the weld. Furthermore, to evaluate the implications to sound propagation, the elastic stiffness encountered by a wave must be known.

The initial use of the electron back-scatter diffraction (EBSD) technique for the quantification and mapping of austenitic weld microstructure for inspection design was recently presented in the 10th ECNDT conference by Carpentier et al [1]. The EBSD technique implemented in a scanning electron microscope is widely used to determine the microtexture of crystalline materials. The crystallographic orientation of the entire weld cross-section at several lengthwise positions was mapped using EBSD.

The austenitic weld specimen studied in this paper using an FE modelling approach is the same as the one described in the paper by Carpentier et al. The specimen represents a typical dissimilar joint used for the safe-end in pressurised water reactors (Figure 1). Information related to the grain boundaries (Figure 2) and orientations of the grain microstructure (Table 1) were taken from this paper.

As described by Carpentier et al, the resolution of the data provided by the EBSD scan has been chosen to be in the Rayleigh scattering domain. EBSD data was processed in order to convert the inverse pole figure map given by the EBSD measurement to a unified orientation map (Figure 2) where each area of orientation smaller or equal to  $20^\circ$  difference were regrouped into the dominant orientation. Table 1 shows the ten selected dominant orientations. Finally, the elastic stiffness of the mapped regions has to be determined to accurately model the propagation of a sound wave in the media. The measured stiffness constants for this weld are taken to be  $C_{11}=203.6$  GPa,  $C_{12}=133.5$  GPa and  $C_{44}=129.8$  GPa [2].

**TABLE 1.** The ten dominant orientations used for the weld map; the crystallographic orientations are expressed as three rotation angles about the x, y and z axes of the component reference frame, as required for modelling. (Reproduced with permission from TWI)

Colour	$\alpha(^{\circ})$ (rotation about x)	$\beta(^{\circ})$ (rotation about y)	$\gamma(^{\circ})$ (rotation about z)
Red	0	0	0
Blue	0	0	45
Lime green	318.72	6.37	193.09
Yellow	12.55	28.25	18.91
Cyan	8.17	4.52	338.91
Brown	30.81	-13.14	29.96
Pink	348.11	-22.77	177.97
Green	21.73	-1.78	8.36
White	351.5	-22.86	138.12
Black	19.95	-1.16	56.60

## FE SIMULATION OF WELD INSPECTION

As the structure of the medium under investigation becomes increasingly complex in composition, analytical and semi-analytical models for simulating ultrasound propagation no longer offer an accurate solution in a reasonable solution time. Indeed, unfeasibly long computational time is often a deterrent for the application of FEA to such a problem. However, as the PZFlex code [3] is specifically designed to model large wave propagation problems with difficult media, the hindrance of an excessively long solve time no longer becomes an issue. Analytical models also have difficulty in dealing with heterogeneous materials as many material boundary conditions presented to the ultrasound path require a unique solution. Again, for an FE simulation, this type of problem poses little or no overhead in terms of solution complexity or time.

From the EBSD scan described in the previous section, a series of discrete crystal orientations can be selected during post-processing and used to identify macro-regions of the weld that similar in behaviour, i.e. any structure within  $\pm 20^\circ$  of the dominant orientation is classed as having the same orientation. This enables a color-coded map to be generated where each color pertains to a particular crystal orientation in a 3 axis system, as shown in Figure 2. As the stiffness matrix for the crystal is known, using PZFlex it is then possible to rotate this matrix to the discrete orientations extracted from the EBSD scan. This results in each color/material having a unique set of material properties, which in turn represents the anisotropy in the simulation. The model is then meshed for an element size that is below the Rayleigh scatterer limit of  $300\mu\text{m}$  and is sufficient for wave propagation accuracy at target frequencies (typically in PZFlex, element size is equal to the shortest wavelength/15). In this case element size is set to  $200\mu\text{m}$  to satisfy both criteria. The final model is approximately 300,000 elements in size and is a 2D plain strain model.

As PZFlex is a transient solver, it is possible to extract time-domain signals from the simulation in similar manner in which one would extract information for a real scan, i.e. A-scan data. This capability facilitates the simulation of an entire inspection, including the phased array probe, complete with individually addressable elements.

The configuration considered in this simulation is the inspection of the butt weld (anisotropic weld described in previous section) in a large diameter pipe filled with water. A  $0^\circ$  beam is generated using an array transducer in contact on the weld surface with the cap being flushed flat as shown in Figure 3. The material on each side of the weld is represented as stainless steel, although any material choice could be implemented provided its properties are known. In relative terms the water load is assumed to be infinite as in practice the pipe diameter would be large compared to the weld thickness. The weld has a 3mm diameter side drilled hole in it to act as a defect. In addition, a model representing an isotropic load (stainless steel) was also created for comparison and was subject to the same procedures as the weld case.

The phased array probe is a linear piezoceramic array with a lossy backing applied. The backing is assumed to be perfect in nature with no reflections generated at the boundary condition. In practice this wouldn't be the case, however, it is a very reasonable assumption to make in this investigation in order to reduce spurious signals in the simulation. Each element is individually addressable allowing the user

to apply any delay laws desired. The probe is designed to have a centre frequency of 1.5 MHz, with each element being 0.5mm wide, 1.2mm thick, with 0.5mm of medium set polymer separating each ceramic pillar. The frequency was chosen from evaluation of the transmission spectra at 4 angles through the weld. In theory the inspection frequency is chosen to be as high as possible in order to provide good spatial and temporal resolution for flaw detection and characterisation. However, Figure 4 shows that for a frequency above 1.5MHz the loss in signal amplitude is too severe for adequate signal over noise ratio (SNR). The sound was generated with a single cycle sine wave excitation pulse with amplitude of 1Vpp.

Using this arrangement, the model was configured in a Full Matrix Capture mode, in which each array element will in turn act as a transmitter with the remainder of the elements in reception until the complete set of transmit/receive pairs is obtained. Considering an array comprising  $n$  elements,  $n^2$  datasets will result. In effect, when applying the FMC technique in this simulation, each transmitting element can be effectively decoupled from one another as the system is time-invariant, resulting in 128 discrete, independent simulations that can be modelled separately and, if necessary, in parallel.

The total run-time for each transmitting element was around 40secs on a quad-core Dell T5500 workstation with 12GB of RAM. The complete set of transmitters providing the FMC data-sets took approximately 90 minutes running sequentially, which means that the entire inspection could be run in around 1minute if parallelised. The signal amplitude on 128 elements for each model was extracted to be used for post-process imaging algorithms on a different system. Given the full matrix of data from a test piece it is possible to implement in post-processing any number of array imaging algorithms. In particular the application of the *total focusing method* (TFM) which allows for focusing of the array at every point in the test-piece in order to form the image and has been shown to outperform all other linear imaging algorithms [4]. Furthermore, TFM can be employed beyond obtaining positional information from a reflector in the test-piece – both scalar and vector functions can be obtained in order to describe a defect's position, orientation and specularity.

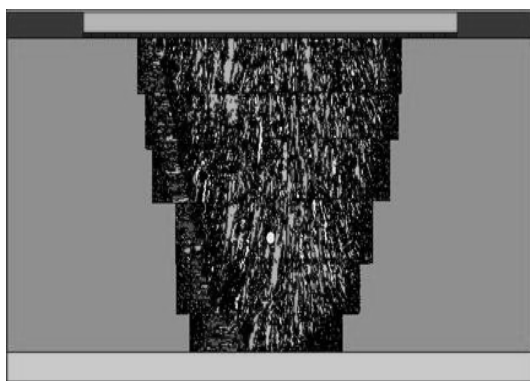


**FIGURE 3.** Full FE model showing the austenitic weld map with 3mm SDH defect and 128 element piezoelectric array on top.

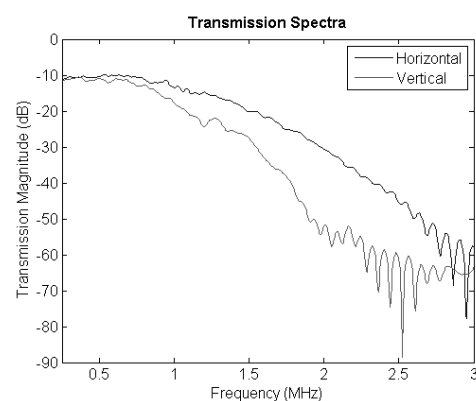


**FIGURE 4.** Through transmission spectra in both the horizontal and vertical directions revealing the anisotropy of the weld and the optimal inspection frequency of 1.5MHz

## SIMULATED INSPECTION RESULTS

The FMC data was read into Matlab, and then processed using the TFM algorithm to produce images of the simulated weld. Firstly, an accumulator array was set up to store the value of each pixel in the image. Then the time of flight from the array elements to each pixel in the image was calculated, and stored in a look-up table. The data was then prepared by taking the Hilbert transform of each individual record in the FMC, resulting in a complex representation of the waveform.

Conceptually, the algorithm steps through every pair of transmit-receive elements, and within this, every pixel in the image. It calculates the cumulative round trip delay along each sound path using the data in the lookup table, then adds the ring-up time associated with the transducer to create a total delay. The complex value at this time in the transmit-receive record is then added to the relevant pixel value in the accumulator array. This process continues until all transmit-receive records have been considered, and the magnitude of the accumulator array is taken to produce an image of the weld. In practice the algorithm was vectorised to make it more efficient. For each transmit-receive pair, all pixels are considered in parallel, avoiding the overhead associated with an additional for loop. As a result each 42,000 pixel image took only 60 seconds to process on a dual core E6750 desktop, with 3GB of RAM.

To allow for comparisons the simulated inspection was also completed for an isotropic load with the same SDH defect present. Figure 5 shows the TFM image generated for this simulation with a 40dB threshold, where the SDH is clearly visible and well resolved. The comparative result for the anisotropic weld assuming a constant wave speed for plotting the data is shown in Figure 6. The important points to note in this image are the decreased single amplitude of 20dB around the defect and also the poorer resolution due to the distortion of the sound energy in the weld. Interestingly, the as the TFM algorithm focuses on each point in the image, the grain interfaces in the weld can be clearly seen albeit their relative position will be skewed due to incorrect delays being applied.

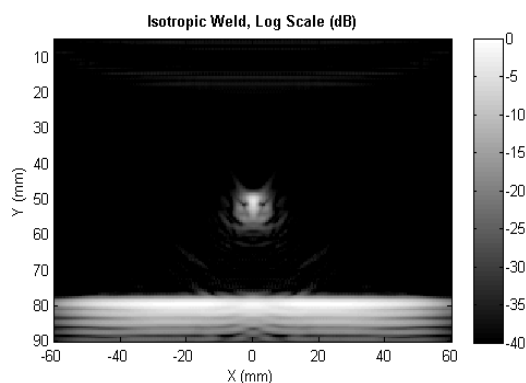


**FIGURE 5.** Imaging results employing TFM on 128 element array operating using FMC on an isotropic sample with 3mm SDH. 40dB threshold applied.

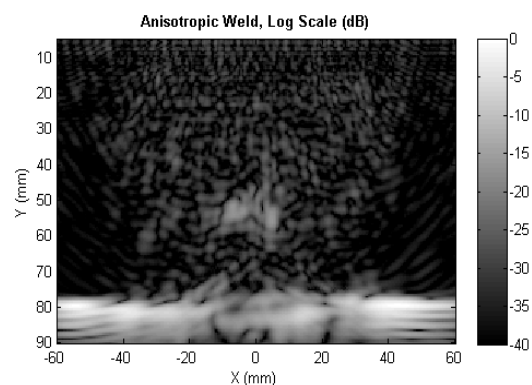


**FIGURE 6.** Imaging results employing TFM on 128 element array operating using FMC on an anisotropic sample with 3mm SDH. 40dB threshold applied.

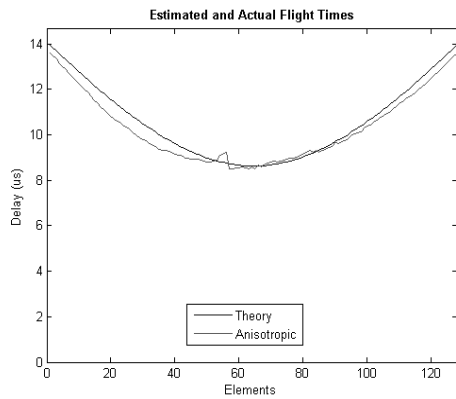


**FIGURE 7.** Delay aberrations from time-reversal anisotropic FE model (green), and theoretical values (blue).

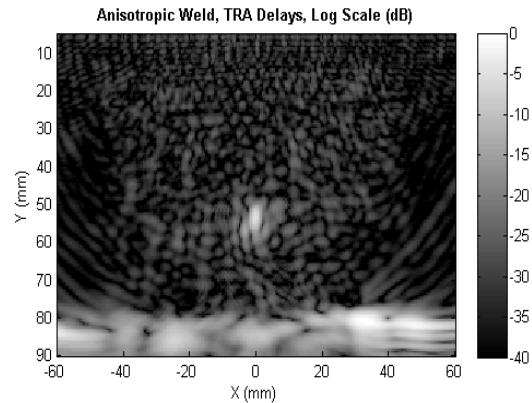


**FIGURE 8.** Imaging results employing TFM with TRA calculated delay laws on 128 element array operating using FMC on an anisotropic sample with 3mm SDH. 40dB threshold applied.

The error in the delay laws obviously causes distortion of the image, as shown in Figure 6; however, these can be corrected for using a simple variation of Time Reversal Acoustics (TRA) in the simulation. By treating the defect as cylindrical source, the precise delays to each element can be calculated from the element receive A-scans. These delays can then be reversed and applied to the elements in order to create a focus at the target. Figure 7 presents the delays from the defect to all 128 elements for the anisotropic weld and the theoretical values for an isotropic media. As is clear from the figure, the TRA delay laws for the anisotropic case deviate from those used in previous TFM results, although it is reasonable to state that the variation is not as large as expected. Nevertheless, the application of the correct delays causes a significant improvement in both defect resolution and sensitivity, as shown in Figure 8. This improvement, however, does not carry over to the backwall wall reflection as the corrected delays are solely for generating a focus at the region of interest.

The correlation between TRA corrected TFM images for the anisotropic weld and that of isotropic case becomes more evident when a 20dB threshold is applied to both sets of data, primarily to remove the reflections from the grain boundaries. This is clearly demonstrated in Figures 9 and 10, where the defect is restored to a level close to the isotropic case in both resolution and amplitude. This shows how TRA methods help to concentrate sound energy at the target, improving signal amplitude and resolution.

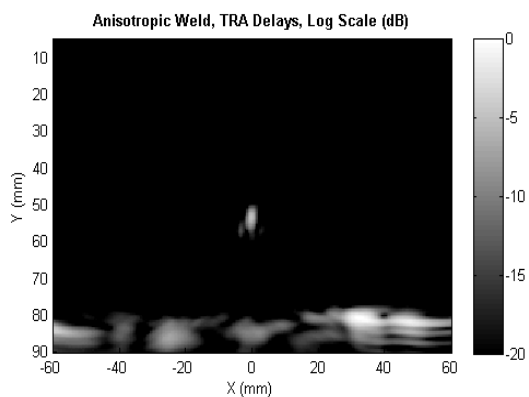


**FIGURE 9.** Imaging results employing TFM with TRA calculated delay laws on 128 element array operating using FMC on an anisotropic sample with 3mm SDH. 20dB threshold applied.

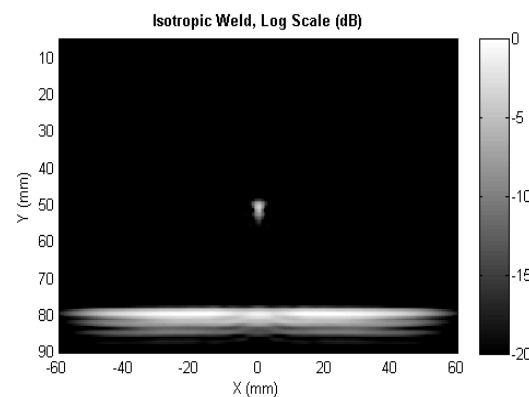


**FIGURE 10.** Imaging results employing TFM (no TRA delay laws applied) on 128 element array operating using FMC on an isotropic sample with 3mm SDH. 20dB threshold applied

## CONCLUDING REMARKS

This paper has described the use of FE via the PZFlex code to simulate the complete inspection of a practical anisotropic weld with a 3mm diameter defect inserted. The weld has been characterised through EBSD scanning. Inspecting such welds with conventional inspection techniques based on ideal delay laws invariably results in poor defect resolution, location, and sizing. An alternative approach is described here whereby a FMC inspection is simulated with a 128 element piezoelectric linear array. This provides a matrix of 128x128 traces that facilitates the implementation of a TFM algorithm. By using TFM to focus on every point in the image, the defect can be clearly identified in comparison to the ideal isotropic case. However, the distortion of the ultrasonic energy causes the defect to appear spread over a larger area with a relative drop in amplitude. This has been rectified through application of a simplified method of TRA that compensates for the distorted delays and creates a focus at the region of interest. This theoretical investigation indicates that TRA compensated TFM inspections can produce images of similar quality to those achieved in an isotropic material by the same inspection method. These results obtained through theoretical approach demonstrate the capability of the FE modelling via PZFlex to simulate advanced phased array techniques for the inspection of austenitic weld and compensate for the weld distortion. However the validation of these results through comparison with experimental data will have to be undertaken in order to establish the degree of accuracy of this theoretical approach before being applied in industry.

## REFERENCES

1. C Carpentier, C Nageswaran and Y Y Tse: 'Evaluation of a new approach for the inspection of austenitic dissimilar welds using ultrasonic phased array techniques', Proc 10th ECNDT conference, Moscow, June 2010.
2. Lenkkeri J and Juva A: 'The effect of anisotropy on the propagation of ultrasonic waves in austenitic stainless steel', Reliability of Ultrasonic Inspection of Austenitic Materials, Belgium, 1980.
3. PZFlex, Weidlinger Associates Inc, 399 W El Camino Real, Mountain View, CA 94040-2607.
4. C. Holmes, B. W. Drinkwater, and P. D. Wilcox, "Postprocessing of the full matrix of ultrasonic transmitreceive array data for non-destructive evaluation," *Nondestr. Test Eval. Int.*, vol. 38, no. 8, pp. 701–711, (2005).